Size-dependent structural and electronic properties of Ti_n clusters ($n \leq 100$)

2007 J. Phys.: Condens. Matter 19 106207

(http://iopscience.iop.org/0953-8984/19/10/106207)

IOP PUBLISHING JOURNAL OF PHYSICS: CONDENSED MATTER

J. Phys.: Condens. Matter **19** (2007) 106207 (18pp) doi:10.1088/0953-8984/19/10/106207

Size-dependent structural and electronic properties of Ti_n clusters ($n \leqslant 100$)

Jan-Ole Joswig[1] **and Michael Springborg**[2]

[1] Physikalische Chemie, Technische Universität Dresden, D-01062 Dresden, Germany
[2] Physikalische und Theoretische Chemie, Universität des Saarlandes, D-66123 Saarbrücken, Germany

E-mail: jan-ole.joswig@chemie.tu-dresden.de

Received 30 November 2006
Published 16 February 2007
Online at stacks.iop.org/JPhysCM/19/106207

Abstract

The results of a genetic-algorithms search for structures of titanium clusters with up to 100 atoms are presented. An empirical pair potential has been used in describing the interatomic interactions during the genetic-algorithms search. The resulting global-minimum structures have been used as starting geometries of geometry optimizations using a density-functional tight-binding method. Structural, energetic, and electronic properties are analysed and compared. Special attention is paid to the size dependence of the properties, including point groups, radial atomic distributions, bond lengths, moments of inertia, stability, Mulliken populations and frontier orbitals. Similarity functions are defined to facilitate the analysis of the growth of the clusters. It turned out that the empirical potential favours highly symmetric geometries, that exhibit small distortions upon relaxation using the electronic-structure method. Some larger, particularly stable clusters are fragments of the hcp bulk structure but an overall transition to bulk structure cannot be seen below 100 atoms.

1. Introduction

Metal-containing clusters are intensively investigated either as free clusters or deposited or grown on surfaces (see, e.g., [1]). Thereby, the size dependence of the properties gives access to information about the growth processes taking place when clusters are formed. The main questions in this context are as follows. Is there a particular cluster size at which a transition to bulk structures takes place? Are there highly symmetric clusters and do they have any specific properties? Which are the corresponding magic numbers and why do these magic clusters exist?

To throw more light on some of these questions we have investigated a series of titanium clusters. Titanium is an early transition-metal element. The main interest so far has been paid to the later transition metals such as Ni, Cu, Au, Ag, Pt, and Pd. However, since the 1990s

Ti_n clusters have come more into the focus of research. A few theoretical investigations have been presented on single, highly symmetric clusters, e.g., the icosahedral Ti_{13} and Ti_{55} clusters, and on clusters with $n < 20$ employing density-functional-based methods [2–6]. The latter interest, however, may be more a limitation regarding computational effort and, moreover, due to the problem of choosing starting structures for larger clusters for which highly symmetric structures can not necessarily be assumed. These studies concentrate mainly on the structural and electronic properties, but present in addition some information about the size dependence of these properties. However, the size range that is covered is rather small so that the present study is—to our knowledge—the first theoretical investigation of size-dependent properties over a wide range of Ti_n clusters with up to $n = 100$ atoms that is continuous over this size range.

For the sake of completeness we add that there has been a number of theoretical and experimental studies dealing with the Ti_2 dimer, e.g., among others the work of Bauschlicher *et al* [7]. In addition, there exists a limited number of publications reporting experimental results for series of titanium clusters. These cover a much larger range of mass-selected cluster sizes with up to more than 100 atoms and present exclusively results deduced from photoelectron spectroscopy [5, 8, 9] except for a study by Sakurai and co-workers [10] who presented time-of-flight mass spectra of clusters with up to 30 atoms. Although these studies give much insight into the optical and other properties of the studied clusters, the overlap between theory and experiment is still very low due to limitations on both sides. We hope that with this study we may contribute to the understanding of nanostructured materials and increase the overlap between experimental and theoretical approaches.

For theoretical calculations of clusters the question how to choose a starting geometry becomes increasingly important with increasing cluster size. Whereas it is possible to guess initial geometries for clusters with up to, say, ten atoms or those whose numbers of atoms suggest that there might be a highly symmetric structural isomer, it is nearly impossible to use human intuition to generate reasonable starting structures for larger clusters. One common approach to deal with this problem is to use the concept of simulated annealing to find the global total-energy minimum structure of the system of interest. Alternatively, so-called genetic algorithms [11, 12] are often used. This is also the method that has been applied to obtain the results of this study.

Nevertheless, even when using such intelligent methods for unbiased structure optimizations, additional problems occur for systems with n, the number of atoms, being just some few tens of atoms. For these, the combination of an essentially exponentially growing number of local total-energy minima with n and of computational needs for the calculation of the total energy of just a single structure that grows with n to some power larger than 2 makes it impossible to use highly accurate total-energy methods for larger ranges of cluster sizes without imposing serious constraints on the sizes and/or structures that shall be studied. Alternatively, one may apply simple empirical approximations to the total energy, which is the most commonly used approach when studying whole series of clusters with more than, say, 20 atoms. However, almost exclusively all such empirical potentials depend on only the interatomic distances, i.e., $E_{\mathrm{tot}} = E_{\mathrm{tot}}(\{r_{ij}\})$ (with r_{ij} being the distance between the ith and the jth atom), whereby directional interactions (through electronic bonds) are excluded.

Although such approaches may provide useful information for the development of the properties of the clusters as a function of size, it is unclear to what extent the neglect of electronic degrees of freedom affects the conclusions. It is the purpose of the present study to address this issue. Thus, by first using one method that excludes the electronic degrees of freedom in optimizing the structures unbiasedly and, subsequently, using another method that includes electronic orbitals in locally relaxing the structures, we obtain estimates on the

importance of directional interactions through electronic orbitals. Moreover, the combined study will provide a much more detailed insight into the properties of the clusters at hand, i.e., Ti_n clusters, than would have been the case for each study, separately.

2. Computational methods

The study presented in this paper has been undertaken using two computational methods, separately. We performed genetic-algorithms calculations for each value of n in Ti_n ($n \leqslant 100$) and, afterwards, the resulting lowest-energy structures were taken as the starting geometries for calculations with a density-functional tight-binding method. We will describe both methods only briefly below.

Genetic algorithms (GAs) are based on the principles of natural evolution [11, 12]. They have been found to provide an efficient computational tool for global geometry optimizations [13–16]. However, genetic algorithms in combination with electronic-structure calculations are computationally heavy and, therefore, we have, in one set of calculations, used an empirical pair potential for the description of the interatomic interactions.

Our GA has originally been developed to deal with two-component clusters [17, 18]. It is able to use two different types of so-called mating procedures to create new clusters which both have been used during the calculations with equal weight.

Generally, in each generation a population of N independent clusters is kept. N should be chosen due to computational possibilities. A large N increases the accuracy of the search on the potential energy surface but also increases the computational time. In our case we performed the calculations using $N = 10$. For each of the N clusters a starting geometry of n atoms is chosen randomly with only minor constraints, i.e., the atoms are forced to lie within a specified volume to ensure interactions between them and no two atoms are allowed to be closer than a certain minimum distance.

After this initial step, the N clusters are relaxed to their nearest total-energy minimum using the pair potential described below. These relaxed clusters are called 'parents'.

The third step is the mating procedure. We used both a single-parent and a two-parent mating procedure. In the first—similar to Jackson's single-parent evolution approach [19]—each of the N clusters is cut randomly (and separately) into three parts. Thereby, the planes of the two cuts are parallel. The two outer parts are then rigidly interchanged. The two-parent mating procedure cuts two cluster structures into parts of m and $(n-m)$ atoms and interchanges the appropriate parts.

After either of these procedures, N newly generated clusters (called 'children') are relaxed to their closest total-energy minimum. Out of the pool of N parent clusters and N child clusters the N clusters with the lowest total energies are selected to build up the parent pool of the next generation.

This procedure is repeated for several hundred generations until the lowest total energy is unchanged for 100 generations. To increase the certainty of having found the global-minimum structure several independent runs were performed so that between 10^4 and 10^5 structures have been generated and relaxed for each cluster size. Nevertheless, there is no absolute certainty—especially for larger clusters—that the resulting cluster is the one of the global total-energy minimum, but, hopefully, it is a very good approximation to it.

For the calculation of the interatomic interactions we used an empirical pair potential given by Cleri and Rosato [20] whereby the cohesive energy of the system is written as

$$E_c = A \sum_{j>i}^{n} e^{-p\left(\frac{r_{ij}}{r_0}-1\right)} - \sum_{i}^{n} \sqrt{\sum_{j\neq i}^{n} \xi^2 e^{-2q\left(\frac{r_{ij}}{r_0}-1\right)}}. \quad (1)$$

Here, r_{ij} is the interatomic distance between the atoms i and j, and r_0 is the nearest-neighbour distance in the bulk crystal lattice. The repulsive part E_{R}^i, which is a sum of Born–Mayer ion–ion repulsions, contains, furthermore, the parameter p that is related to the compressibility of the bulk metal. The band-energy term E_{B}^i contains an effective hopping integral ξ and the parameter q that describes the dependence on the relative interatomic distance.

The parameters have been determined through fitting to experimental bulk values by Cleri and Rosato [20] and for the sake of completeness we include their values for titanium here: $A = 0.1519$ eV, $\xi = 1.8112$ eV, $p = 8.620$, $q = 2.390$, and $\beta = 1.5874$. The latter is used to calculate $r_0 = a_0 \cdot \sqrt{\frac{1}{3} + \frac{\beta^2}{4}}$ with $a_0 = 2.9508$ Å.[3]

In our second set of calculations, performed with the purpose of getting information on the importance of electronic degrees of freedom, the global-minimum structures described by the empirical potential were subsequently refined using a parameterized density-functional tight-binding (DFTB) method [21–23].

This method is based on the density-functional theory of Hohenberg and Kohn [24] in the formulation of Kohn and Sham [25]. The total energy of the system of interest relative to the isolated atoms is written as

$$E_{\mathrm{T}} = \sum_i \epsilon_i - \sum_{jk} \epsilon_{jk} + \frac{1}{2} \sum_{k \neq l} U_{kl}(|\mathbf{R}_k - \mathbf{R}_l|), \tag{2}$$

where ϵ_i is the Kohn–Sham eigenvalue of the ith orbital of the system and ϵ_{jk} is the energy of the jth orbital of the isolated atom k. U_{kl} is a pair potential between the atoms k and l.

The single-particle Kohn–Sham eigenfunctions $\psi_i(\mathbf{r})$ are expanded in a set of localized atom-centred basis functions $\varphi_m(\mathbf{r})$. These functions are determined by self-consistent density-functional calculations on the isolated atoms employing a large set of Slater-type basis functions.

The effective one-electron potential in the Kohn–Sham Hamiltonian is approximated as a superposition of the atomic potentials of the corresponding neutral atoms. Moreover, only two-centre integrals are calculated to set up the Hamilton matrix. Finally, all electrons except for the 4s and 3d electrons were treated within a frozen-core approximation.

3. Results

First, we will investigate the energetic stability of the Cleri–Rosato (CR) and the DFTB clusters. Therefore, we show in figure 1 the stability function which is defined as $E_{\mathrm{stab}}(n) = E_{n-1} + E_{n+1} - 2E_n$ with E_k being the total energy of the k-atomic cluster.

The stability function of the CR clusters shows maxima at $n = 13$, 19, 38, 46, 49, 55 and further maxima above $n = 70$ in fairly regular intervals. After applying the DFTB scheme and re-optimizing the clusters with the electronic-structure method the stability function changes significantly. The function shows a few significant peaks. The most stable clusters are now those with $n = 19$, 38, 48, 67, 70, 73, whereby the three latter are the most prominent peaks. The neighbouring clusters ($n = 66$, 68, 69, 74) are particularly unstable.

Some of these magic numbers arise from geometrical shell closings and correspond to highly symmetric structures such as, e.g., Ti_{13} (icosahedron), Ti_{19} (double-icosahedron), Ti_{38} (truncated octahedron), and Ti_{55} (Mackay icosahedron). These clusters are most stable within the CR series. However, if electronic effects are taken into account through DFTB, other clusters arise as stable structures, e.g., Ti_{67}. A significant change happens to Ti_{13} and Ti_{55} that show only small peaks in the DFTB stability function.

[3] The parameter a_0 has been corrected according to Kittel [28], since it has been misprinted in [20].

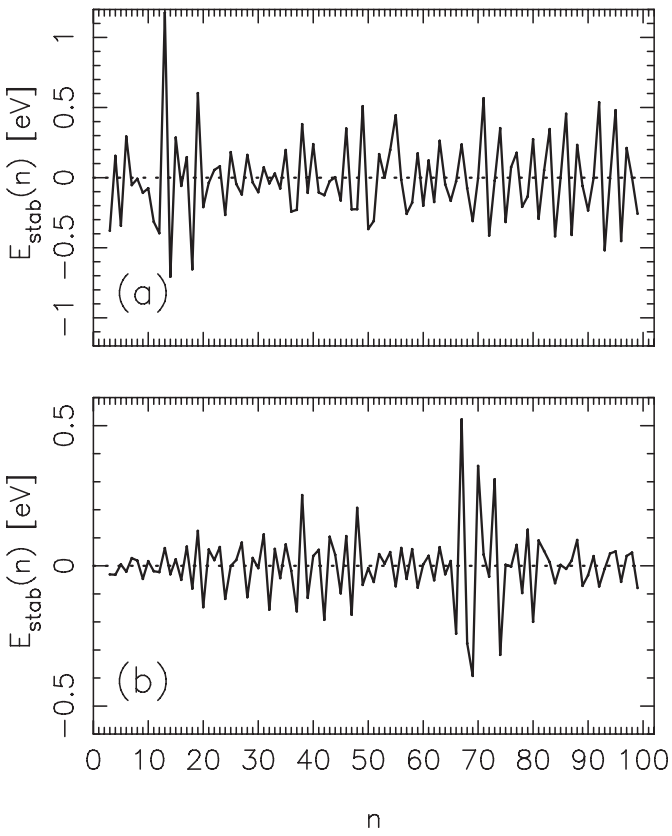

Figure 1. Stability functions of the titanium clusters described by (a) the CR and (b) the DFTB potential as functions of cluster size. The stability function is defined as $E_{\mathrm{stab}}(n) = E_{n-1} + E_{n+1} - 2E_n$ with E_k being the total energy of the Ti_k cluster. Note the different scaling of the y axes.

The stability of a series of titanium clusters with up to around 30 atoms has been investigated experimentally by Sakurai and co-workers [10] using time-of-flight mass spectrometry. The authors found the Ti_n clusters with $n = 7$, 13, 15, 19, 25 to show the highest abundances. Moreover, in their spectra Ti_{23} has an abundance comparable to that of Ti_{25}, so we can include this cluster into the list as well. Comparing these numbers to figure 1 we find agreement for $n = 13$, 15, 19, 23, 25 for the CR clusters and for $n = 7$, 13, 15, 19, 23 for the DFTB clusters. For the DFTB clusters these stability peaks are rather small. Sakurai *et al* propose icosahedral structures or other five-fold symmetries for these clusters, except for Ti_{15}, to which they assign a bcc structure. However, the authors did not obtain these geometries directly from their mass spectra. In particular, the proposed bcc structure is in contrast to our findings (cf figure 2(a)), whereas we find structural agreement for the clusters with $n = 7$, 13, 19. In our calculations a Ti_{15} cluster with bcc structure is 0.6 eV higher in energy (within the CR description) than the structure we found, which is a doubled hexagonal bipyramid. Also the DFTB optimization of the bcc structure results in this geometry.

Another study of the stability of titanium clusters has been published by Zhao and co-workers [3], who found the 7- and 13-atom clusters to be magic. Also in the most recent density-functional study on Ti_n clusters, by Salazar-Villanueva *et al* [6], these two cluster sizes were found to be particularly stable. Compared to the stability functions in figure 1

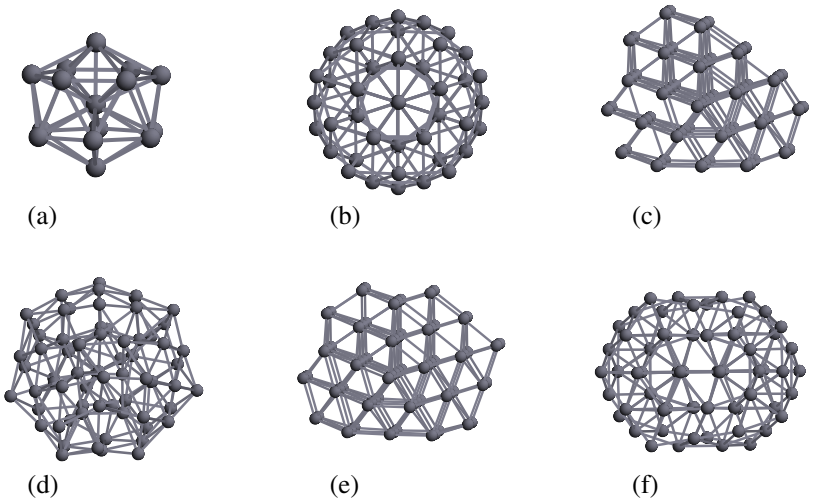

Figure 2. Cluster structures of (a) Ti_{15} (CR), (b) Ti_{55} (CR), Ti_{67} (DFTB), Ti_{68} (DFTB), Ti_{73} (DFTB), and Ti_{74} (DFTB).

we can confirm this only for the DFTB series. Within the empirical cluster series only Ti_{13} is energetically favoured.

Figure 3 shows the radial distribution of the atoms as a function of cluster size for both series. The radial distribution is defined as follows. For each atom of a Ti_n cluster, we calculate the distance to the centre of mass, $r_i = |\mathbf{R}_i - \mathbf{R}_0|$, with

$$\mathbf{R}_0 = \frac{1}{n}\sum_{i=1}^{n}\mathbf{R}_i \tag{3}$$

and $\mathbf{R}_i$ being the position of the ith atom. Subsequently, all these n distances per cluster are shown as a function of cluster size n. In the size-dependent radial distribution of the CR clusters (figure 3(a)) we can see that the radius which is approximately given by the largest radial distance possesses an overall increase. However, at certain sizes the radius decreases with increasing cluster size, e.g., at $n = 36$, 37, 44, 59, 60, 73, 83, 89. Moreover, at certain sizes higher symmetric clusters can be identified. These show only a few different distances, because several atoms are located at symmetrically equivalent positions. This is the case for, e.g., $n = 38$, 51–55, 67, 74, 90–92.

A third feature obtained from figure 3 is the occurrence of atomic shells. From $n = 10$–12, a single inner-shell atom appears. This is the inner atom of the icosahedron ($n = 13$) whose second (outer) shell is built up from $n = 10$–13. From $n = 19$ onwards, the inner shell consists of more than one atom, and the third shell appears at $n = 51$. The radial distances of the different shells are well separated in the diagram and, thus, we can follow the building-up of new shells easily.

By comparing the two diagrams in figure 3 it can be seen that the overall structure is conserved during relaxation of the geometries with the DFTB method, because the two diagrams look very similar. The main difference between the two series is that within the DFTB description the clusters are slightly expanded. Furthermore, larger clusters tend to show a less symmetric radial distribution. Thus, although the electronic degrees of freedom are important for many details, as we shall see below, their importance is not sufficiently strong to be clearly recognizable in figure 3.

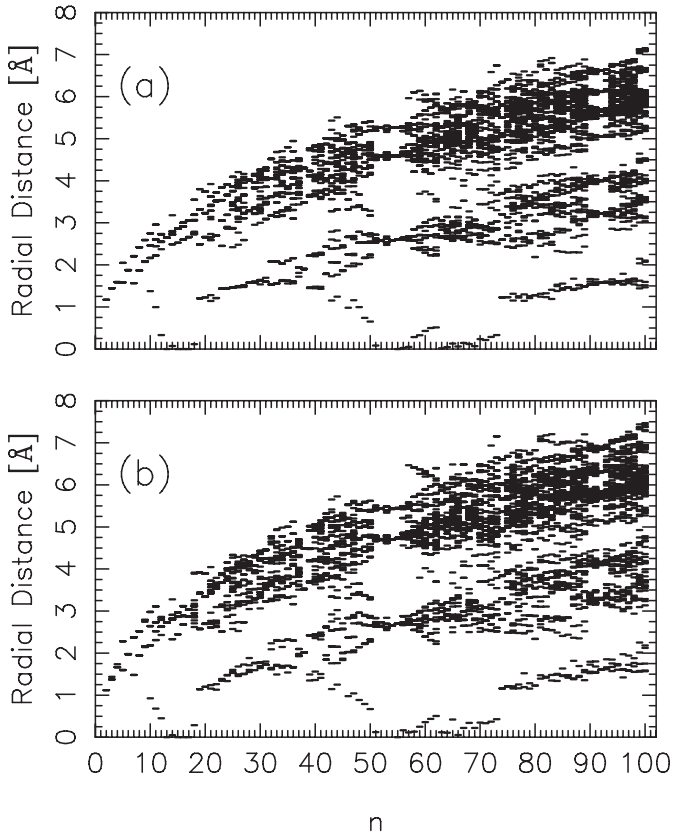

Figure 3. Radial distributions of the atoms as a function of cluster size of (a) the CR and (b) the DFTB cluster series. Each horizontal line represents the distance of one specific atom to the centre of mass. Several lines may lie on top of each other if the corresponding atoms have the same radial distances.

In figure 4 we show the average bond length as a function of cluster size as well as the minimum bond length in each cluster. Moreover, we compare in table 1 the average bond lengths for some small clusters with *ab initio* results. For the calculation of the average bond length we have defined bonding to take place at interatomic distances below 3.20 Å. This is an arbitrary value that is, however, significantly larger than the titanium bulk bond length of 2.90 Å [26]. The average bond lengths for clusters with more than 70 atoms are around 2.77 and 2.85 Å for CR and DFTB clusters, respectively, and, thus, both are close to the bulk value of 2.90 Å.

The minimum interatomic distance in each cluster is shown as the dotted curve in each diagram of figure 4. The DFTB curve shows some strong outstanding peaks for $n = 38$, 46, 48, 52–55, 67, 70, 71, 73. Some of these numbers correspond to clusters with particularly high symmetries ($n = 38$, 54, 55), because the minimum distance and the average bond length are nearly the same. The symmetries can be deduced from the point groups which are presented in table 2. The clusters below 25 atoms possess particularly high symmetries. Above 25 atoms these high-symmetry point groups appear less often except for, e.g., Ti_{38} (O_h), Ti_{54} and Ti_{55} (I_h), and Ti_{74} (D_{3d}). The clusters with more than 80 atoms have nearly exclusively a very low symmetry. Table 2 also shows the point groups of the DFTB clusters explicitly, if they differ

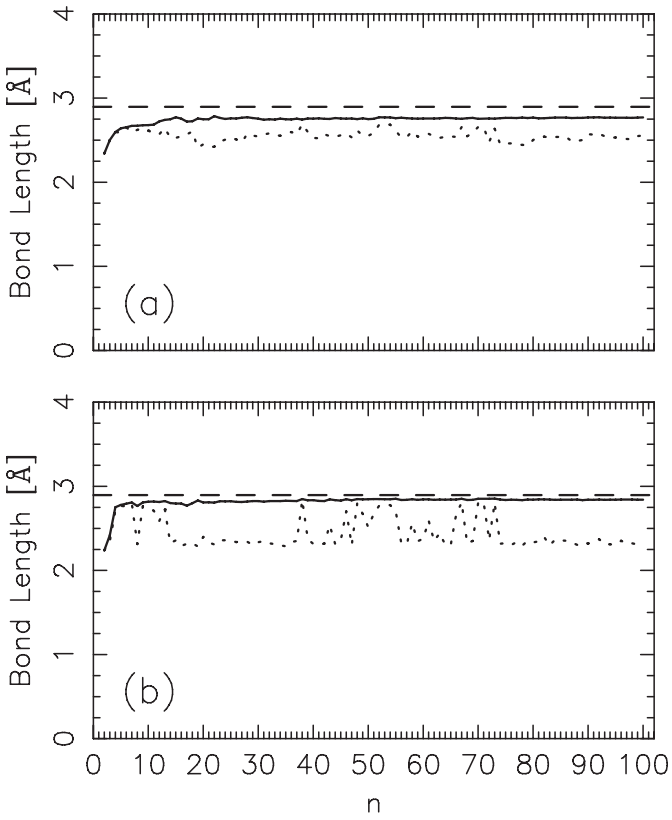

Figure 4. Average bond length (solid lines) and minimum bond length (dotted lines) of (a) the CR and (b) the DFTB cluster series as functions of cluster size. The horizontal dashed lines show the experimental value of the bond length (2.90 Å) [26].

Table 1. Average bond lengths in Å. Structural isomers are chosen from the reference studies according to DFTB geometries (cf table 2).

n	CR	DFTB	[2]	[3]	[6]
2	2.34	2.24	1.94	1.93	1.97
3	2.50	2.42	2.40	2.28	2.21
4	2.60	2.75	2.52	2.51	2.49
5	2.64	2.78	2.48	2.54	2.49
6	2.65	2.79	2.68	2.62	2.64
7	2.67	2.81	2.63	2.62	2.63
8	2.67	2.77	2.65	2.63	

from the CR point groups. We can observe that one third of the investigated structures show distortions upon geometry optimization with the DFTB method. The recent density-functional study on Ti_n clusters with $n \leqslant 15$ by Salazar-Villanueva *et al* [6] predicted in general structures of a higher symmetry than those we have found with the DFTB method.

Bauschlicher *et al* [7] have calculated the bond length of the Ti_2 dimer in the $^3\Delta_g$ state (later assigned to be the ground state) [27] to be 1.97 Å, which is in agreement with the experimental value of 1.94 Å ($^3\Delta_g$) measured by resonant two-photon ionization

Table 2. Point groups (marked PG) of the investigated Ti_n clusters. If only one point group is stated, it refers to both the CR and DFTB clusters. Otherwise, the first point group refers to the CR, and the second to the DFTB cluster. An asterisk marks the point groups of strongly distorted cluster structures.

n	PG	*n*	PG	*n*	PG	*n*	PG
2	$D_{\infty h}$	27	C_s	52	D_{5d}	77	C_1
3	D_{3h}/C_{2v}	28	T/C_1	53	C_{5v}	78	C_1
4	T_d/C_{3v}	29	C_3	54	I_h/I_h^*	79	C_s
5	D_{3h}	30	C_s/C_1	55	I_h/I_h^*	80	C_2
6	O_h/D_{2h}	31	C_3	56	C_{3v}	81	C_1
7	D_{5h}	32	D_3/C_1	57	C_s	82	C_s
8	D_{2d}	33	C_2/C_2^*	58	C_{3v}	83	C_s
9	D_{3h}	34	C_s	59	C_s	84	C_1
10	C_{3v}	35	C_{2v}	60	C_s/C_s^*	85	C_1
11	C_{2v}	36	C_2	61	C_{2v}	86	C_3/C_1
12	C_{5v}^*	37	C_s/C_s^*	62	C_1	87	C_1
13	I_h/D_{3d}	38	O_h/O_h^*	63	C_{2v}	88	C_1
14	C_{2v}	39	C_5	64	C_s	89	C_1
15	D_{6d}/D_{2d}	40	C_s/C_1	65	C_1	90	C_1
16	D_{3h}	41	C_s/C_1	66	C_1	91	C_1
17	T_d	42	D_2/C_2	67	C_{2v}	92	T/D_2
18	C_{2v}	43	C_s	68	C_1	93	C_3/C_1
19	D_{5h}/C_{2v}	44	C_s	69	C_2/C_2^*	94	C_1
20	D_{3d}/D_{3d}^*	45	C_2/C_1	70	C_s	95	C_3/C_1
21	C_s	46	C_{2v}	71	C_{2v}	96	C_1
22	D_{6h}/C_1	47	C_1	72	C_1	97	C_1
23	D_{3h}/C_{2v}	48	C_{2v}	73	C_s	98	C_1
24	D_3/C_2	49	C_{3v}/C_s	74	D_{3d}/D_{3d}^*	99	C_1
25	C_3/C_1	50	C_s	75	C_2	100	C_1
26	C_1	51	C_{2v}	76	C_1		

spectroscopy [27]. The dimer bond lengths calculated with CR and DFTB are 2.33 and 2.23 Å, respectively. Although these values are rather large, compared to the experiment or full DFT calculations, the bulk bond length is described very well within DFTB, as we have seen above.

The Ti_n (CR) clusters with $n = 3$–13 show the same geometries as many other clusters described by pair-potentials. They adopt the following structures: equilateral triangle, tetrahedron, trigonal bipyramid, octahedron, pentagonal bipyramid, bicapped octahedron, tricapped trigonal prism. The clusters with 10–12 atoms are parts of the 13-atomic icosahedron.

In the DFTB series the cluster structures are generally the same, but show small distortions. These structures are consistent with the structures presented by Castro *et al* [5], Salazar-Villanueva *et al* [6] (except for Ti_9), Wei *et al* [2] (for $n = 3$, 4, 5, 7). The latter studies have calculated different structural isomers for each cluster size, whereas in this work we have taken the CR structures as a defined starting point. We have summarized the bond lengths of these cluster structures in table 3 for comparable geometries. As mentioned above, the bond length in the dimer is too large for both the CR and DFTB clusters. But with increasing cluster size the CR and DFTB bond lengths approach the *ab initio* values.

For the icosahedral Ti_{13}, Wang *et al* [4] find the distorted D_{3d} structure to be most stable. We observe this distortion in the DFTB series as well, but the CR cluster has of course I_h symmetry. The bond lengths given in [4] are 2.567 and 2.699 Å (I_h isomer) and 2.580–2.695 Å (D_{3d} isomer). For the CR cluster we observe 2.63 and 2.77 Å and for the distorted DFTB isomer 2.72–2.87 Å. The agreement with other *ab initio* results is, thus, better for larger clusters than

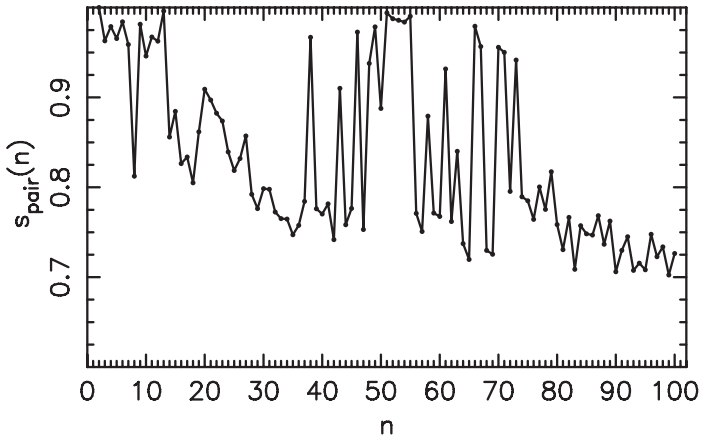

Figure 5. Similarity function s_{pair} that measures the similarity of the CR and the DFTB clusters by comparing the interatomic distances in each cluster (defined in (4)). For two identical clusters the similarity function will be 1 whereas for two structurally very different clusters it will approach 0.

Table 3. Bond lengths (in Å) of the two cluster series compared to the work of Castro *et al* [5].

n	CR	DFTB	[5]
2	2.33	2.23	1.902
3	2.49	2.34, 2.43, 2.46	2.35, 2.35, 2.44
4	2.58	2.70, 2.78	2.48, 2.57
5	2.58, 2.73	2.76, 2.78	2.45–2.59
6	2.64	2.75–2.81	2.57–2.68
7	2.58–2.70	2.78–2.79	2.55–2.62
8	2.61–2.75	2.30–2.82	2.57–2.71

for the dimer. But despite the deviation of around 5% we can observe the distortion from I_h to D_{3d} symmetry.

In order to study whether the structures of the two approaches are similar or not, we define the following similarity function $s_{\text{pair}}(n)$: we calculate all $n(n-1)/2$ interatomic distances d_{ij} between any two atoms i and j in the two clusters with the same number of atoms, sort them, and use

$$\frac{n(n-1)}{2} q_{\text{pair}}^2 = \sum_{i>j=1}^{n} \left(\frac{d_{ij}^{\text{CR}}}{d_0^{\text{CR}}} - \frac{d_{ij}^{\text{DFTB}}}{d_0^{\text{DFTB}}} \right)^2 \tag{4}$$

to obtain the so-called pair-distribution similarity function $s_{\text{pair}}(n) = (1 + q_{\text{pair}})^{-1}$. Thus, two identical clusters will result in a value of $s_{\text{pair}}(n) = 1$ whereas for two structurally very different clusters the similarity function will approach 0.

In (4), the superscripts CR and DFTB indicate that the variables refer to the CR and DFTB cluster series and d_0 is the minimum bond length in the corresponding clusters. The division by the latter assures that the function is independent of bond-length variations and only compares the geometries.

The resulting diagram is depicted in figure 5. The curve is overall decaying. There are, however, several peaks that indicate a particularly high similarity between the corresponding clusters, e.g., at $n = 13$, 38, 46, 49, 51–55, 66, 67, 70, 71, 73 and—with slightly smaller values—for $n = 20$, 43, 58, 61, 63. For these numbers the DFTB relaxation of the CR cluster

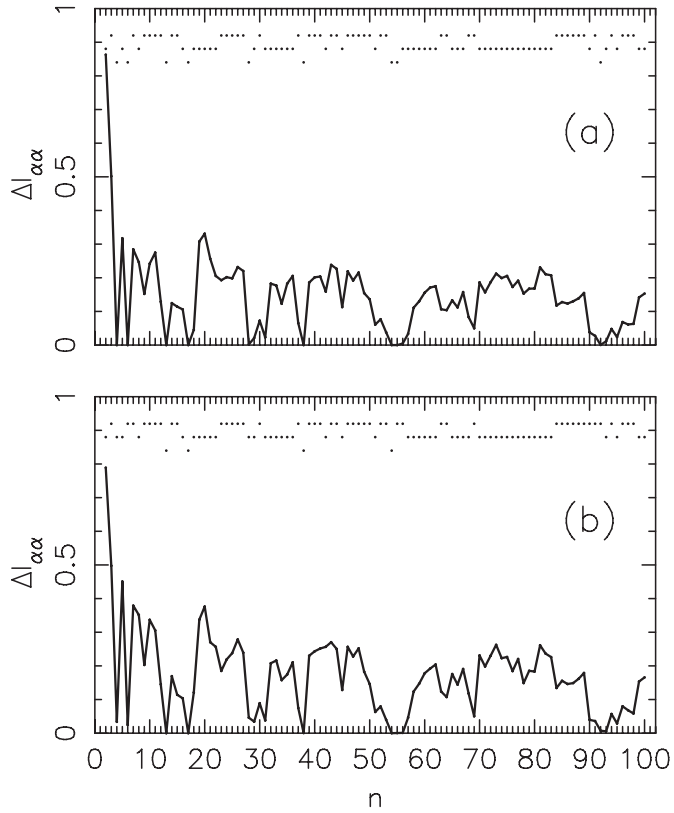

Figure 6. The normalized difference $\Delta I_{\alpha\alpha}$ of largest and lowest eigenvalue of the matrix containing the moments of inertia as a function of cluster size for (a) the CR and (b) the DFTB cluster series. In the upper part of each panel, a simple estimate of the overall shape of the clusters is given, either being spherical (marked with points in the lowest row), cigar shaped (points in the middle row), or lens shaped (points in the uppermost row).

structure does not change the geometrical structure. Scaling effects are excluded, as mentioned above. For other clusters, stronger structural deformations occur. These do not necessarily have to involve changes of the geometry. The similarity function just shows which clusters are less affected by the DFTB relaxation. In other words, the minima on the two potential energy surfaces correspond, if $s_{\text{pair}} = 1$.

By comparing the maxima of s_{pair} with those of the stability function (cf figure 1) we see a correspondence between stable clusters (within both series) and high similarity for most of these structures. We can conclude that the most stable clusters are geometrically already well described by the empirical CR potential (excluding scaling). We may also conclude that geometrical packing effects are the major contributions to the energetics of these clusters. In contrast, for those clusters with a low value of s_{pair}, geometrically favourable packing is difficult to achieve and, thus, the CR and DFTB descriptions result in less similar, distorted structures.

Besides the similarity, the overall shape of the two cluster series may shed light upon the cluster growth. Therefore, we calculate for a given n-atomic cluster the eigenvalues $I_{\alpha\alpha}$ of the matrix containing the moments of inertia $\sum_{i=1}^{n} s_i t_i$. Herein, s_i and t_i are the x, y, and z coordinates of the atom i in a coordinate system centred at the centre of mass $\mathbf{R}_0$ (defined in (3)). For a spherical jellium $I_{\alpha\alpha} \propto n^{5/3}$, and therefore we show in figure 6 the difference

between the largest and the lowest eigenvalues $\Delta I_{\alpha\alpha} = |I_{\alpha\alpha}^{\max} - I_{\alpha\alpha}^{\min}|/n^{5/3}$ for each series as a function of n. If $\Delta I_{\alpha\alpha} = 0$, all three eigenvalues are identical, and the overall shape of the cluster is approximately spherical. These clusters are marked with points in the lowest row of the upper part of the diagrams. Spherical clusters are found for $n = 13$, 17, 38, 54 in both series and, additionally, for $n = 4$, 6, 28, 55, 92 in the CR series. Here, we see that a distortion towards lower symmetries (cf table 2) is caused by the DFTB relaxation.

Clusters marked with a point in the middle row of the upper part of the diagrams of figure 6 have two small eigenvalues and one large eigenvalue, i.e., they are essentially prolate (cigar shaped). Those clusters that have one small eigenvalue and two large eigenvalues are oblate (lens shaped) and marked with points in the uppermost row. Comparing both diagrams we see periods of constant shapes with increasing number of atoms, especially above 20 atoms. These constant periods are even more distinctive in the DFTB cluster series (figure 6(b)). This may suggest that in these size ranges the clusters grow by adding atom by atom to a certain core.

In order to address this question further, i.e., whether a cluster consisting of n atoms can be considered as resulting from a cluster with $(n-1)$ atoms plus an additional single atom, we define the similarity function s_1. We calculate the $(n-1)(n-2)/2$ interatomic distances d_{ij}^0 for the cluster with $(n-1)$ atoms and sort them. Subsequently, we consider all possible $(n-1)$-atomic parts of the n-atomic cluster, i.e., n different parts of each $(n-1)$ atoms, and also calculate and sort their interatomic distances d_{ij}. The smallest value of q_1 with

$$\frac{(n-1)(n-2)}{2} q_1^2 = \sum_{i>j=1}^{n-1} \left(\frac{d_{ij}^0}{d_{\min}^0} - \frac{d_{ij}}{d_{\min}} \right)^2 \tag{5}$$

defines the similarity function of the n-atomic cluster, $s_1(n) = (1+q_1)^{-1}$. Similarly as above, the function is 1 for a cluster that is obtained by adding a single atom to the $(n-1)$-atom cluster, and approaches 0 for very different structures.

Figure 7 shows the resulting functions for the CR and the DFTB cluster series. In general the similarity function of the empirical clusters has values much closer to 1. This means that the CR structures are often more related to each other than in the DFTB series. The reason is certainly the above-mentioned structural distortion within the DFTB series. However, there are some values of n where the function approaches 1, e.g., for $n = 52$–55, 71, and several clusters with more than 80 atoms. In the DFTB series, the similarity function shows these features even more distinct.

Finally, we will discuss the similarity between the clusters and cutouts of the bulk crystal lattice, in order to see whether a transition to bulk structures is observable. Titanium crystallizes in hcp structure [26] and, therefore, we define a similarity function that measures the similarity between the clusters and an hcp cutout. This is done as follows. A sufficiently large cutout is taken as reference and the distance of every atom to a chosen origin is calculated. Similarly, we calculate the radial distances (r_i of atom i) in every cluster of each series and, finally, compare both sets of distances (n distances for each Ti_n cluster) within

$$n q_{\mathrm{hcp}}^2 = \sum_{i=1}^{n} \left(\frac{r_i}{d_0} - \frac{r_i^{\mathrm{hcp}}}{d_0^{\mathrm{hcp}}} \right)^2 \tag{6}$$

where d_0 is the minimal interatomic distance in both systems (as explained above) and the superscript hcp indicates that the corresponding values are taken from the hcp cutout. Finally, the similarity function is defined as $s_{\mathrm{hcp}} = (1+q_{\mathrm{hcp}})^{-1}$.

Figure 8 shows the resulting curves as functions of n for both series. Furthermore, for each series four different curves have been calculated corresponding to four different origins of the hcp cutout. Thereby, the origin was moved from (000) to three other high-symmetry points

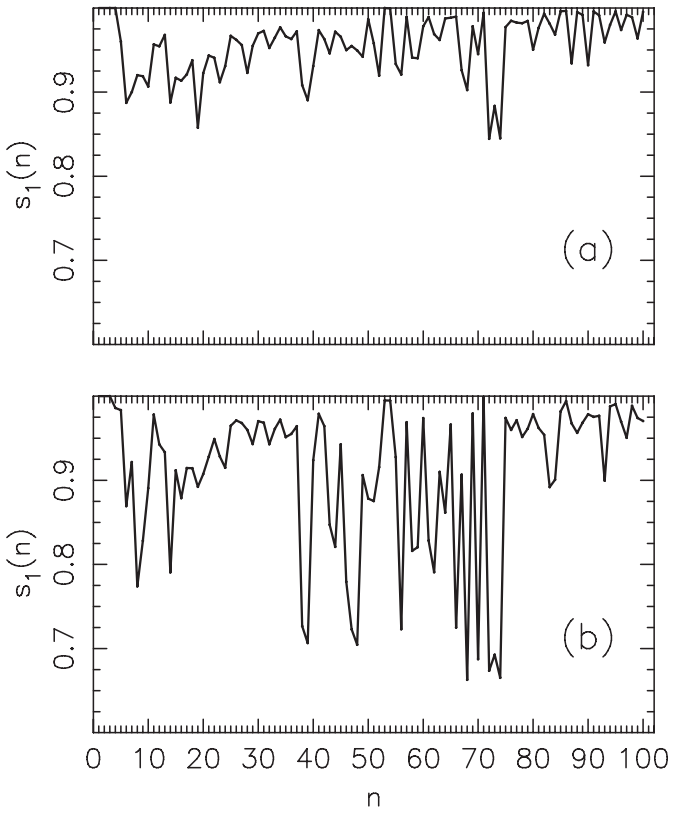

Figure 7. Similarity function s_1 of (a) the CR and (b) the DFTB cluster series. s_1 gives the similarity between the n-atomic cluster and one of its $(n-1)$-atom parts and is defined in (5).

of the hcp unit cell (at $(\frac{1}{2}00)$, $(0\frac{1}{6}\frac{1}{4})$, and $(\frac{1}{2}\frac{1}{4}0)$). The resulting functions do obviously not show significant differences. For both series the curves run parallel, but for the DFTB clusters they lie essentially on top of each other for clusters with more than 50 atoms. Overall the CR clusters (especially the larger ones) show a much higher similarity with the hcp fragment than the DFTB clusters, whereas in both series there are some prominent peaks at the same cluster sizes, e.g., for $n = 67$, 70, 71, 73 atoms. Here it should be remembered that the hcp structure is a closed-packed structure and that the CR potential implicitly favours closed packing.

As we have already observed in figure 1, these four clusters are exceptionally stable in the DFTB series. Here, we find a strong correlation between the stability and the bulk hcp structure. Moreover, Ti_{67}, Ti_{70}, and Ti_{73} do not have a high similarity function regarding their $(n-1)$-atomic parts (cf (5) and figure 7). The most stable clusters in this size region are, therefore, not structurally related to each other but consist of (differently centred) hcp fragments. This can be verified by having a look at the cluster structures which are presented in figures 2(c) and (e). The structures with $n = 66$, 68 (cf figure 2(d)), 69, 72, 74 (cf figure 2(f)) which show less similarity with the hcp fragment have indeed more spherical structures. Hereby, Ti_{68} is low-symmetric (C_1), whereas Ti_{74} is of high symmetry (D_{3d}).

Although the hcp structure seems to be energetically favoured from certain sizes onwards, the major part of the clusters does show lower values of the similarity functions and the structures tend to exhibit triangular faces and a clear shell structure.

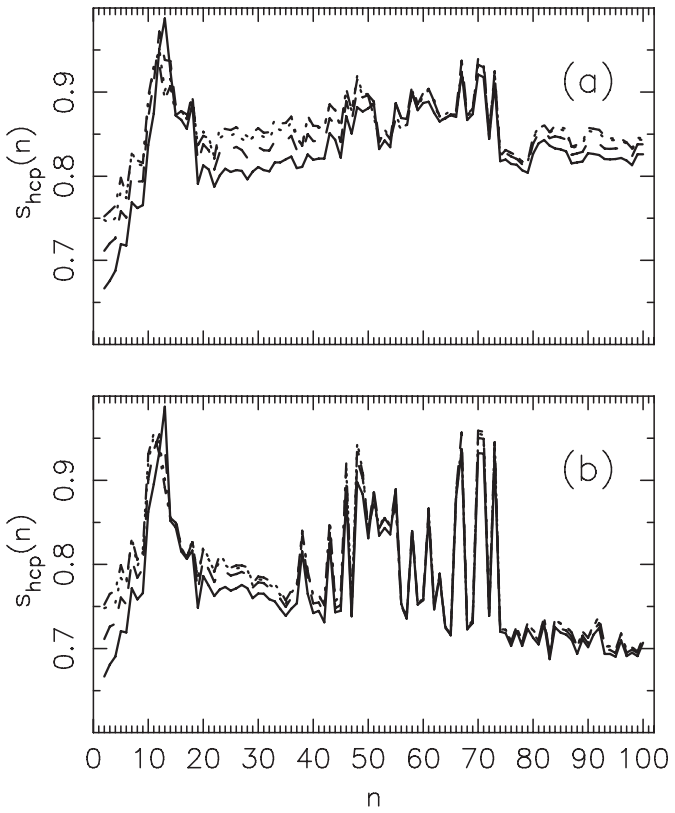

Figure 8. Similarity functions s_{hcp} quantifying the similarity of (a) the CR and (b) the DFTB clusters with a cutout of an hcp crystal. The four curves in each panel correspond to an atom in the hcp crystal sitting at positions (000) (solid), $(\frac{1}{2}00)$ (dotted), $(0\frac{1}{6}\frac{1}{4})$ (dashed), and $(\frac{1}{2}\frac{1}{4}0)$ (dotted–dashed). This function is defined in (6).

Liu *et al* [8] showed in an experimental study of clusters with up to 130 atoms that in this size regime the clusters have in general no bulk structure. This is consistent with our findings as we have found hcp bulk fragments to be stable only in a few cases. Because the surface-to-bulk ratio is very large for clusters with fewer than 100 atoms, the transition to bulk structures will probably first take place for much larger clusters.

Moreover, we still can find five-fold symmetry in these structures which is a remainder from icosahedral growth. In this size regime these two growth patterns (icosahedral versus hcp) are both present and occurring simultaneously in the same cluster.

Finally, we discuss electronic properties that have been obtained through the density-functional calculations. Figure 9 shows the gap between highest occupied and lowest unoccupied molecular orbital (HOMO/LUMO gap) as a function of cluster size. We show this both for the CR structures (described by DFTB) and the fully relaxed DFTB structures.

We observe that both curves decay rapidly and approach a nearly zero band gap within the first 20 atoms. The values of the HOMO/LUMO gap of the larger clusters above 50 atoms are without exception below 0.03 eV. Although this is below the accuracy of our method, the strong trend towards metallic behaviour can be seen. We add that the HOMO/LUMO gaps reported by Salazar-Villanueva *et al* [6] are very similar to the present ones.

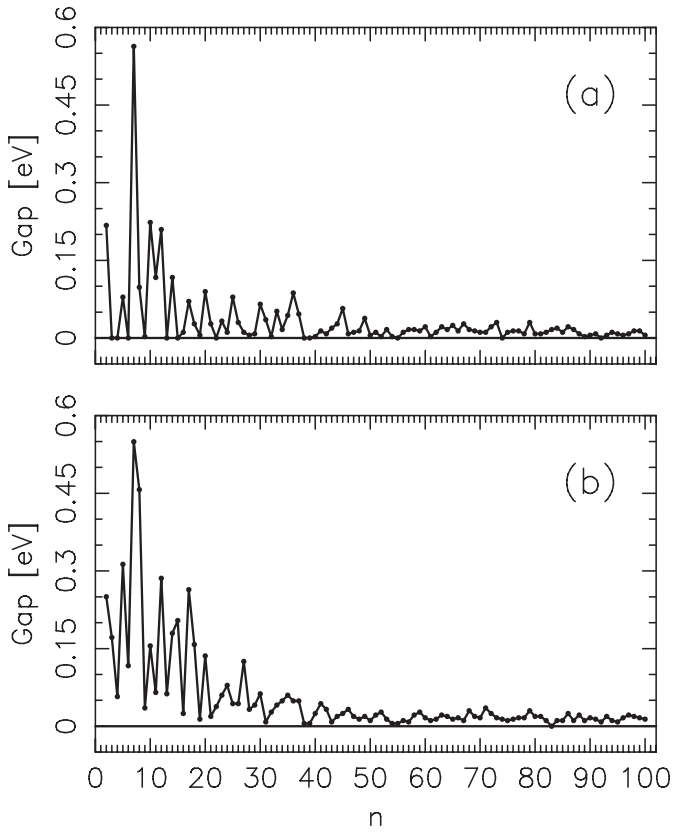

Figure 9. HOMO/LUMO gaps of (a) the CR geometries and (b) the fully relaxed clusters of the DFTB series as functions of cluster size.

Moreover, for $n < 20$ a gap opens up for some clusters due to the relaxation, a typical sign for Jahn–Teller distortions which we observed above. The most outstanding example in this sense is Ti_8, for which the gap increases by 0.3 eV. We can see from figure 5 that this cluster shows a strong distortion compared to the initial CR structure.

In their theoretical work, Zhao and co-workers [3] proposed that titanium clusters show (electronic) bulk properties from Ti_8 onwards. However, as they have used Gaussians (width 0.1 eV) to broaden their density of states, this may suggest an earlier closing of the gap with increasing cluster size. But in any case, we find metallic behaviour occurring latest for clusters between 10 and 20 atoms.

Besides the Kohn–Sham eigenvalues we have access to the Mulliken populations of the atoms. To investigate their size dependence we make use of their radial distribution. For Ti_{100}—a single, but typical case—the radial distribution of the Mulliken gross populations is presented in figure 10(a). For every single atom its radial distance is calculated and at this specific distance a point in the diagram marks its Mulliken gross population. Comparing all the populations to the number of valence electrons (marked as a horizontal dashed line in the diagram) strong charge transfers within the cluster can be seen. Hereby, those atoms with small radial distances, i.e., the inner shell atoms, have the highest populations whereas the surface atoms (those with large distances to the origin) have the smallest populations.

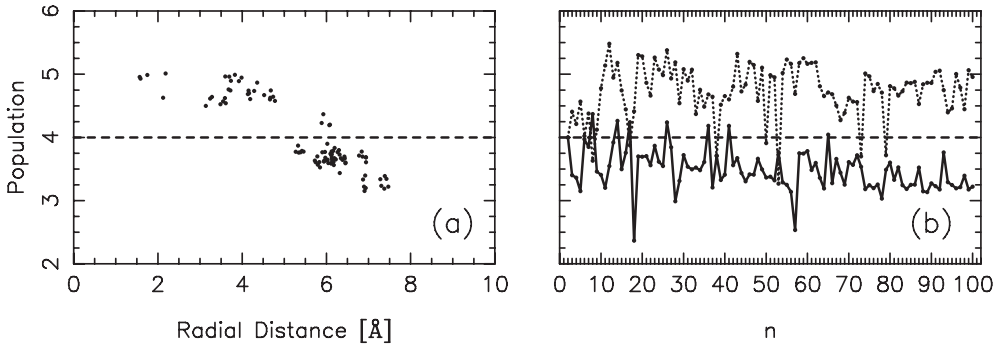

Figure 10. (a) Radial distribution of the Mulliken gross populations in Ti_{100}. The centre of mass is at $x = 0$. Each point represents the Mulliken population of a single atom, whereby the x value gives its distance to the centre of mass. On the y axis the Mulliken gross population is marked. (b) Mulliken populations of the atoms with largest distance to the centre of mass (solid curve) and those with smallest distance to the centre of mass (dotted). The dashed lines in both panels mark the number of valence electrons of a titanium atom which is four.

Ultimately, for very large clusters the central atoms should become neutral, but this limit has clearly not been reached in the present study. We add that the variations in the atomic charges can not be interpreted as due to Friedel oscillations. Assuming a free-electron model with four electrons per atom, the electron-gas parameter becomes $r_s = 0.37$ Å, leading to Friedel oscillations with a periodicity of 0.61 Å, i.e., much smaller than the scale of the oscillations in figure 10(a).

This trend of charge transfer from surface atoms to inner (bulk) atoms can be seen in nearly all clusters. To visualize it we show in figure 10(b) for each cluster the Mulliken gross population of the two atoms with largest (solid line) and smallest distance to the centre of mass (dotted line) as a function of cluster size (i.e., for each cluster the population of an inner-shell atom and a surface atom is given). If we neglect the clusters with fewer than 20 atoms the surface atoms in every cluster lose electrons (there are still some exceptions in clusters with 30–40 atoms) whereas the inner atoms gain electrons. Thus, for the clusters of the present study, the Mulliken populations of the surface atoms approach 3 with increasing cluster size (and, thus, have a positive Mulliken charge), whereas those of the inner atoms have populations around 5 (negative Mulliken charge).

4. Conclusions

In this study we have investigated the size-dependent properties of two continuous series of titanium cluster structures which have been obtained by a genetic-algorithms search using an empirical pair potential and additional density-functional tight-binding calculations of the resulting cluster structures. Although we cannot be sure that we have found the global-minimum structures in all cases we hope at least that the genetic-algorithms search resulted in good approximations to them. Since it is very difficult to choose 'good' initial geometries for large systems we believe that this approach is reasonable and consequential to get information on large cluster series and their properties.

We found the highly symmetric clusters to be particularly stable within the empirical potential. Within the DFTB series some other clusters turned out to be most stable, especially those that showed a high similarity to bulk fragments with hcp structure. These clusters also showed the highest similarity between the two series. We conclude therefore that they are

geometrically well described by the empirical potential and only scaled during the DFTB relaxation.

The size-dependent radial distribution showed a shell-building very clearly. From 10 atoms onwards the clusters have two atomic shells; from 51 atoms onwards they consist of three shells.

The point groups show particularly high symmetries for the smaller clusters with up to 25 atoms, but large clusters with more than 80 atoms have mainly C_1 symmetry. The DFTB relaxation leads generally to a geometrical Jahn–Teller distortion.

The HOMO/LUMO gap is very small, decreases very rapidly with increasing cluster size, and approaches a nearly zero gap at latest for clusters with 10 to 20 atoms. However, we can just indicate a trend here, since we reach the limit of accuracy of our method. The Mulliken populations show that electronic charge is transferred from the surface to the bulk part of the clusters in the size range we have considered.

Finally, by comparing the results of the DFTB calculations with those of the CR calculations, it is clear that even for a system like Ti_n clusters, electronic degrees of freedom may have impacts on the energetic and structural properties that are of relevance, at least for a detailed description of the cluster properties.

We believe that we have given some insight into the size dependence of cluster properties, especially by the definition of the functions that we used throughout this investigation. Furthermore, we have shown that a combination of approximate empirical potentials with electronic-structure methods may be one way of getting information of large, but finite systems. As we have seen, a quantum-mechanical description of these systems is indeed necessary. Finally, we emphasize that many of the conclusions of our work were obtained through application of various analysing tools that we have devised explicitly for this purpose.

Acknowledgments

One of the authors (MS) is grateful to Fonds der Chemischen Industrie for very generous support. Furthermore, this work was supported by the DFG through the SFB 277 at the University of Saarland.

References

[1] Baletto F and Ferrando R 2005 *Rev. Mod. Phys.* **77** 371
[2] Wei S H, Zeng Z, You J Q, Yan X H and Gong X G 2000 *J. Chem. Phys.* **113** 11127
[3] Zhao J, Qiu Q, Wang B, Wang J and Wang G 2001 *Solid State Commun.* **118** 157
[4] Wang S-Y, Duan W, Zhao D-L and Wang C-Y 2002 *Phys. Rev.* B **65** 165424
[5] Castro M, Liu S-R, Zhai H-J and Wang L-S 2003 *J. Chem. Phys.* **118** 2116
[6] Salazar-Villanueva M, Hernández Tejeda P H, Pal U, Rivas-Silva J F, Rodríguez Mora J I and Ascencio J A 2006 *J. Phys. Chem.* A **110** 10274
[7] Bauschlicher C W Jr, Partridge H, Langhoff S R and Rosi M 1991 *J. Chem. Phys.* **95** 1057
[8] Liu S-R, Zhai H-J, Castro M and Wang L-S 2003 *J. Chem. Phys.* **118** 2108
[9] Wu H, Desai S R and Wang L-S 1996 *Phys. Rev. Lett.* **76** 212
[10] Sakurai M, Watanabe K, Sumiyama K and Suzuki K 1999 *J. Chem. Phys.* **111** 235
[11] Holland J H 1975 *Adaption in Natural Algorithms and Artificial Systems* (Ann Arbor, MI: The University of Michigan Press)
[12] Goldberg D E 1989 *Genetic Algorithms in Search, Optimization and Machine Learning* (Reading, MA: Addison-Wesley)
[13] Deaven D M and Ho K M 1995 *Phys. Rev. Lett.* **75** 288
[14] Poteau R and Pastor G M 1999 *Eur. Phys. J.* D **9** 235
[15] Hartke B 1999 *J. Comput. Chem.* **20** 1752
[16] Roberts C, Johnston R L and Wilson N T 2000 *Theor. Chim. Acc.* **104** 123
[17] Joswig J-O, Springborg M and Seifert G 2001 *Phys. Chem. Chem. Phys.* **3** 5130

[18] Joswig J-O and Springborg M 2003 *Phys. Rev.* B **68** 085408
[19] Rata I, Shvartsburg A A, Horoi M, Frauenheim T, Siu K W M and Jackson K A 2000 *Phys. Rev. Lett.* **85** 546
[20] Cleri F and Rosato V 1993 *Phys. Rev.* B **48** 22
[21] Blaudeck P, Frauenheim T, Porezag D, Seifert G and Fromm E 1992 *J. Phys.: Condens. Matter* **4** 6389
[22] Porezag D, Frauenheim T, Köhler T, Seifert G and Kaschner R 1995 *Phys. Rev.* B **51** 12947
[23] Seifert G, Porezag D and Frauenheim T 1996 *Int. J. Quantum Chem.* **58** 185
[24] Hohenberg P and Kohn W 1964 *Phys. Rev.* **136** B864
[25] Kohn W and Sham L J 1965 *Phys. Rev.* **140** A1133
[26] Pawar R R and Deshpande T 1968 *Acta Crystallogr.* A **24** 316
[27] Doverstål M, Lindgren B, Sassenberg U, Arrington C A and Morse M D 1992 *J. Chem. Phys.* **97** 7087
[28] Kittel C 1966 *Introduction to Solid State Physics* (New York: Wiley)